WELDING RESEARCH

SUPPLEMENT TO THE *WELDING JOURNAL*, APRIL 1992

Sponsored by the American Welding Society and the Welding Research Council

Microstructure and Properties of a Welded Al-Cu-Li Alloy

GTA weldments made with Li-containing filler metals display good properties

BY L. S. KRAMER AND J. R. PICKENS

ABSTRACT. Aluminum-lithium alloys are being considered for several applications that take advantage of the attractive combination of properties in these alloys including low density, high modulus, and high strength. A recently introduced Al-Cu-Li alloy, Weldalite™ 049[1], has the unique combination of ultrahigh strength and good weldability. In this investigation, the mechanical properties of fusion weldments of Weldalite 049 made using Li-containing filler metals are examined. Hardness, tensile tests at ambient and cryogenic temperatures, fractography, and microstructure were evaluated for weldments made with three ternary Al-Cu-Li filler metals and commercial Al-Cu filler metal 2319. The response to heat treatment of these weldments was also investigated. The results suggest that the use of Li-containing filler metals can produce weldments that are free from hot-tearing problems and possess good mechanical properties.

Introduction

The use of lithium-containing aluminum alloys in welded applications has not been widespread in the Western World due to concerns over weldability. In aluminum alloys, hot-tearing resistance is the property that is most often equated with weldability, although other issues, such as pretreatments to prevent porosity and the welding parameters required to obtain good joint strength, are also important.

L. S. KRAMER and J. R. PICKENS are with Martin Marietta Laboratories, Baltimore, Md.

Weldalite™ 049 was introduced in the late 1980s as a high-strength weldable alloy (Refs. 1, 2), whose excellent strength has been attributed to the high Cu:Li wt-% ratio and the addition of minor amounts of Ag and Mg to stimulate precipitation hardening. One of the advantages of this alloy is its ability to attain very high strengths with or without prior cold work, a necessity to attain the highest strength tempers in most Al-Cu and Al-Cu-Li alloys. This, along with a very strong natural aging response (*i.e.*, hardening at ambient temperature) make the alloy attractive for a variety of applications, most notably aerospace applications such as cryogenic fuel tanks for launch systems. The alloy has been welded by various processes, with improvements in joint strengths over those obtained with existing alloys (Refs. 1, 2, 4, 5). The Cu and Li contents of the alloy are such that it is expected to be easily weldable (Ref. 3) and indeed, its weldability, as measured by resistance to hot-tearing was determined to be almost as good as that of the easily welded Al-Cu Alloy 2219, and superior to that of Al-Cu-Li Alloy 2090 and Al-Cu-Mg Alloy 2014 (Ref. 4).

KEY WORDS

GTAW
Li Filler Metal
Al-Cu-Li Alloy
Weldability
Tensile Properties
Hardness
Microstructure
X2094
Weldalite
Heat Treatment

The low-density Li-containing Al alloys such as 2090, 8090 and 2091 were commercially developed to effect fuel cost savings in aircraft. Joining in the aircraft industry is primarily accomplished via mechanical fastening, so weldability was not a primary concern in developing these alloys. The possibility of also using the advantageous combination of aluminum-lithium alloy properties for space applications, where parts are often joined by welding, led to several preliminary weldability investigations of commercial Al-Li alloys (Ref. 5). This research has primarily been concerned with mechanical properties, hot-tearing resistance, choice of filler metal, and corrosion behavior of weldments.

The purpose of this present investigation is to gain a better understanding of the relationship between the microstructure of weldments made with Li-containing filler metals and the mechanical properties. It is hoped that weldments of Li-containing aluminum alloys could be utilized to their full potential by the development of Li-containing filler metals that produce weldments of high strength

[1] *Registered with Aluminum Association in two variants, X2094 and X2095.*

Table 1—Composition of Alloys (wt-%, bal. = Al)

Base Metal	Cu	Li	Other
Weldalite™ 049 nominal[a]	4.75	1.25	0.4 Mg, 0.4 Ag, 0.14 Zr, 0.03 Ti
Filler Metals			
5-0.5 nominal	5.2	0.5	—
measured	5.20	0.47	—
5-1.0 nominal	5.2	1.0	—
measured	5.02	0.95	—
5-1.5 nominal	5.2	1.5	—
measured	5.04	1.39	—
2319 nominal	6.3	—	0.18 Zr, 0.15 Ti, 0.30 Mn, 0.10 V

(a) This composition is within the range of Weldalite™ Alloy X2094, registered with the Aluminum Association.

and ductility without harmful hot-tearing. This investigation focuses on the mechanical properties of weldments at ambient and cryogenic temperatures, and the response of the weldments to heat treatment.

Experimental Procedures

Based on the mechanical properties of Weldalite 049 and its weldability, filler metals with similar high-Cu low-Li contents were chosen as model alloys for investigation. Four filler metals were examined: three ternary Al-Cu-Li alloys and Al-Cu Alloy 2319 — Table 1. Each filler metal was spooled welding wire of 0.0625-in. (1.6-mm) diameter. The base metal used was 0.375-in. (9.5-mm) thick extruded bars of Alloy X2094 in the underaged T8 condition. This was obtained by a solution heat treatment at 500°C (932°F) for 1 h followed by a water quench, cold work (*i.e.*, 3% stretch), and artificial aging at 160°C (320°F) for 6 h.

Variable polarity gas tungsten arc welding (VPGTAW) was used to join two, 2-in. (51-mm) wide extruded bars of X2094-T8. The joint configuration was a flush square-groove butt joint (*i.e.*, no root opening), and the bars were rigidly clamped and welded in the horizontal position with filler metal added through an automated wire feed mechanism. The welding parameters are listed in Table 2. The joint was oriented parallel to the extrusion direction.

Chemical milling in a 30% NaOH aqueous solution at 100°C (212°F) was used to remove the surface layer of the bars and prepare them for welding. The bars were then cleaned in a 30% HNO_3 aqueous solution. Just prior to welding, the joint faces were mechanically abraded with a hand file.

Both Vickers hardness traverses with a 10-kg load and optical microscopy were used to examine the effect of heat input on the different weld zones in the weldment.

Smooth, round tensile specimens (0.25-in./6.3-mm diameter) with a 1.0-in. (25.4-mm) gauge length consisting of the weld, heat-affected zone (HAZ), and base metal were used to minimize the effects of slightly different weld bead geometries. In addition, reduction in cross-sectional area was used as a more sensitive and more representative measure of relative ductility in addition to specimen "apparent" elongation. That is, since plastic deformation was confined to the weld zone, elongation is dependent on specimen gauge length, but reduction in area is not. Weldment tensile specimens were tested at an ambient temperature of 20°C (68°F) and at a cryogenic temperature of –196°C (385°F) attained in a liquid nitrogen bath. Most weldments were tested in the as-welded condition, *i.e.*, only ambient temperature (natural) aging occurred. The response to heat treatment was examined on weldments made using one of the filler metals (5Cu-1Li). Although not practical on many large structures, heat treatment of weldments is sometimes used on small parts or on parts that subsequently undergo a forming operation. Heat treatments examined included postweld artificial, *i.e.*, elevated temperature aging (PWA), and solution heat treatment of the weldment (specimens were solution heat treated similarly to the base metal as outlined above) plus natural or artificial aging, referred to as SHT + NA and SHT + AA, respectively.

Optical metallography was performed on chemically etched specimens (etchant: H_2O + 2 g NaOH + 5 g NaF) and on anodized specimens (Barker's reagent: H_2O + 2 vol-% HBF_4 at 20V) under polarized light. The former etchant clearly shows the microstructural phases, whereas the anodizing technique reveals the grain structure.

Table 2—Fusion Welding Parameters

Current:	235 A	Gas:	He 70 ft³/h (33 L/min)
Voltage:	12.5 V	Electrode:	W (2% Th), 30 deg included angle 0.04 in. (1 mm) truncation
Polarity:	0.01 s electrode negative 0.001 s electrode positive	Travel:	11 in./min (4.6 mm/s)
Frequency:	91 Hz	Wire Feed:	20 in./min (8.5 mm/s)

Results

Weldability

Radiographic investigation of the fusion weldments revealed no hot-tearing (*i.e.*, good weldability), even though the bars were highly constrained during welding. The weldments exhibited a surprisingly bright and clean surface for Li-containing alloys and no appreciable porosity. This can be attributed to three factors:

1) The Li content of this alloy is lower than that of other commercial Li-containing alloys (near 1 wt-% vs. greater than 2 wt-%)

2) The successful surface removal treatment given to the plates prior to welding.

3) The use of a variable polarity power wherein the AC component of the VPGTAW process imparts a cleaning action on the molten weld pool without a significant sacrifice in joint penetration depth.

Hardness

Hardness traverses on the weld and HAZ show little differences, which is likely in part due to the high dilution of base metal into the weld. Based on the measured ratio of the cross-sectional area of the joint before and after welding, it was found that the fusion zone contains 70 to 80% base metal. In general, the first weld pass is somewhat harder than the second, and in the HAZ, hardness first increases, then decreases, and finally increases to the base metal value of approximately 200 VHN. Postweld artificial aging decreases the fusion zone hardness slightly, whereas SHT increases the hardness, as expected, and causes a leveling of the local hardness peak in the HAZ, as shown for the 5Cu-1Li filler metal weldments in Fig. 1.

Tensile Tests

In the as-welded condition, tensile strengths of approximately 50 ksi (345 MPa) with good ductility were obtained for all four weldment variants —Table 3. At –196°C, differences among the variants became apparent, with the 5Cu-1Li filler metal weldments attaining the highest tensile strength: 58.7 ksi (405 MPa) with a 5.4% RA.

The ultimate tensile strength (UTS) was not greatly affected by the PWA, although reduction in the cross-section area (RA) increased in the early stages of aging. Postweld artificial aging may prove to be a simple, practical method for increasing weldment ductility for certain applications. Artificial aging after SHT similarly increased ductility at short aging times with a corresponding strength decrease. With continued aging, tensile strengths as high as 87.8 ksi (605 MPa) were obtained, although ductility decreased at the longer aging times required for such high strength — Table 4. Although the limited amounts of materials available prevented extensive weldment temper development, the preliminary properties presented here are extremely encouraging.

Microstructural Evaluation

Little difference in grain size is observed when comparing weldments made with the Al-Cu-Li filler metals to those made with 2319, even though the 2319 filler metal contains several grain refiners (Zr, Ti, V, Mn) at relatively high levels and the Al-Cu-Li filler metals contain none. Apparently, dilution of base metal into the fusion zone provides sufficient amounts of grain-refining elements (Zr, Ti) to effect grain refinement.

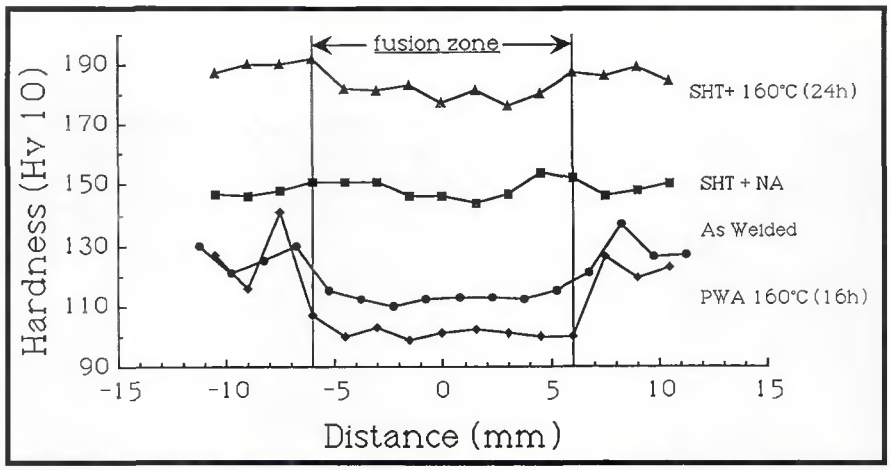

Fig. 1 — Hardness traverses of the 5Cu-1Li filler metal weldment in the as-welded condition and in several heat-treated conditions.

Table 3—Weldment Tensile Test Results, As-Welded Condition[a]

Filler metal	0.2% Y S ksi (MPa)	U T S ksi (MPa)	R A (%)	El (%[b])
at 20°C				
5-0.5	33.8 (233)	48.6 (335)	7.5	3.3
5-1.0	34.7 (239)	49.9 (344)	10.5	3.7
5-1.5	34.5 (238)	50.8 (350)	10.0	4.4
2319	34.4 (237)	49.7 (343)	10.7	3.9
at −196°C				
5-0.5	43.8 (302)	55.7 (384)	4.5	1.8
5-1.0	44.3 (305)	58.7 (405)	5.4	2.6
5-1.5	44.9 (310)	57.4 (396)	2.0	2.0
2319	44.3 (305)	55.7 (384)	3.3	1.7

(a) Each datum is the mean of 3 values.
(b) % elongation in 1 in. (2.54 cm).

Table 4—Weldment Tensile Test Results after Heat Treatment (5-1.0 Filler)

Aging Temp. (°C)	Aging time (h)	0.2% Y S ksi (MPa)	U T S ksi (MPa)	R A (%)	El (%[a])
PWA					
160	2	23.9 (165)	43.3 (299)	19.9	4.9
160	6	26.1 (180)	45.4 (313)	30.7	7.9
160	24	37.0 (255)	50.4 (347)	6.0	2.5
SHT	+				
25 (NA)	700	49.0 (338)	70.1 (483)	20.3	16.9
160	2	39.5 (272)	67.6 (466)	27.6	25.7
160	6	41.8 (288)	66.9 (461)	23.1	20.1
160	16	51.3 (354)	69.6 (480)	17.1	7.8
160	20	65.7 (453)	79.1 (545)	11.6	4.4
160	24	62.7 (432)	74.0 (510)	10.7	3.7
160	40	84.1 (580)	87.8 (605)	2.7	0.8
160	67	83.0 (572)	86.8 (598)	3.2	0.8
180	6	69.1 (476)	73.6 (507)	3.5	0.9
at −196°C, SHT +					
25 (NA)	700	63.9 (441)	80.4 (554)	6.3	9.4
160	20	72.0 (496)	81.8 (564)	5.5	1.9

(a) % elongation in 1 in. (2.54 cm).

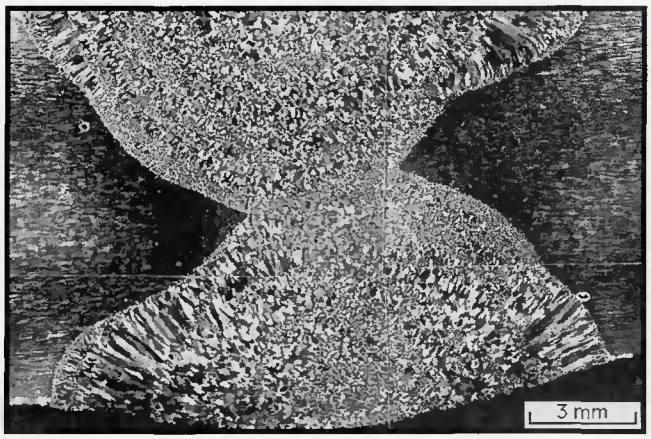

Fig. 2 — Weldment cross-section (filler metal 5Cu-1Li).

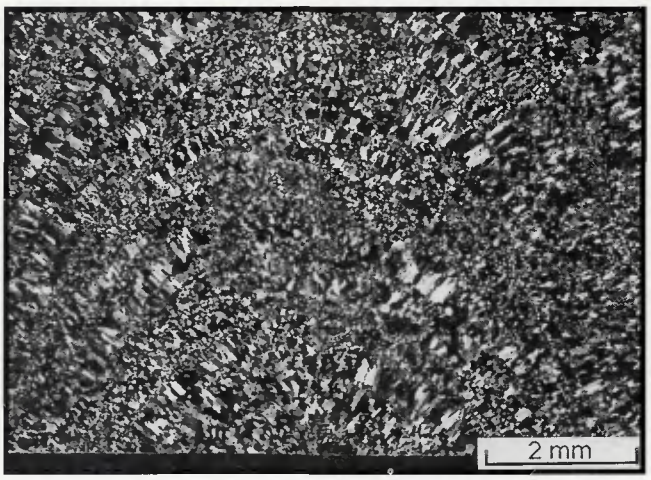

Fig. 3 — Banded grain structure after the first weld pass.

These elements, in the form of intermetallic aluminide dispersoids, act as nucleation sites during solidification, thereby refining grain size (Refs. 6, 7). In addition, disrupted solidification caused by the agitation of the weld pool during welding contributes to the fine grain size observed — Fig. 2.

The first weld pass is generally more refined than the second pass, and transverse solute banding or contouring is apparent in the representative micrographs of Fig. 3. It is likely that fluctuations in the welding arc cause cyclic changes in growth rate at the liquid/solid interface producing bands of solute enrichment and solute depletion, which often leads to bands of different grain sizes (Ref. 8). Each grain contains colonies of dendrites with parallel stems that solidify with few side branches in a structure designated "cellular dendritic."

On the dendrite boundaries, intermetallic phases are present as a result of divorced-eutectic solidification. The fast solidification rate associated with welding, coupled with high interfacial energy, causes the eutectic constituents to solidify in this separated form. After solidification, the solute-rich intermetallic constituent is present in a semiglobular morphology on the cell boundaries with the aluminum solid-solution constituent being indistinguishable from the aluminum matrix.

Discussion

Hardness: As-Welded Condition

Only a small amount of precipitation hardening is possible in the weld zone due to the solute concentration gradient in the grains. Solute concentration varies from the grain interior to the grain boundary due to the nature of dendritic solidification (Ref. 9). As the weld pool solidifies, the first solid consists mainly of α-aluminum, with much of the solute partitioned into the lower melting point liquid and ultimately to the cell boundaries after solidification is complete. The degree of solute segregation is dependent upon alloy composition and cooling rate. The resulting non-uniform, solute-depleted grains have low hardness. In addition, insufficient quenching from welding temperatures apparently results in little supersaturation for precipitation hardening. Microstructural refinement and some type of heat treatment provided by the second pass (*e.g.*, possibly solution treatment or artificial aging) cause the fusion zone from the first welding pass to be somewhat harder than that of the second.

In the HAZ, hardness increases and then decreases with distance from the fusion line — Fig. 1. The portion of the HAZ closest to the weld is harder than the rest of the HAZ, but still softer than the base metal. A possible explanation for this behavior is that this region of the weldment was subjected to sufficient heat for a reasonable amount of solutionizing and a fast enough cooling rate to be quenched and produce a somewhat supersaturated solid solution. Very fine precipitates could have formed during cooling or during natural aging, resulting in a local hardness peak in the HAZ. Such a phenomenon has previously been observed in the HAZ of Al-Cu Alloy 2219 and the similar Russian Alloy 1201 and was attributed to phase dissolution followed by fine θ′ precipitation in this region (Refs. 10, 11). Phases present in the HAZ of Weldalite 049 have not yet been identified but are likely similar to the fine precipitates of δ′ (Al_3Li) and GP zones found in the base metal after quenching (Refs. 12, 13).

Optical micrographs of these regions discussed above are shown in Fig. 4. The cast structure of the weld zone is shown in Fig. 4A, with the region of the HAZ closest to the weld, (corresponding to the high-hardness zone), shown in Fig. 4B. Partial melting, as characterized by pockets of a two-phase eutectic structure is evident in this region. The adjacent softer region of the HAZ etches more readily, and Fig. 4C reveals an overaged microstructure. As the hardness traverse progresses into the base metal, the heat transfer from welding has negligible influence on the base metal microstructure — Fig. 4D.

Hardness: Heat-Treated Conditions

Postweld aging does not affect the hardness greatly for the times and temperatures evaluated. Artificial aging after welding results in an inhomogeneous distribution of precipitates, especially outside the fusion zone, where the base metal was already in the heat-treated T8 condition prior to welding.

Solution heat treatment redissolves most of the interdendritic phases in the fusion zone and the visible phases in the HAZ, and quenching retains a somewhat supersaturated solid solution in the matrix, allowing precipitation hardening to occur upon aging. More solute is available for strengthening in the matrix than on the boundaries because SHT causes the grain interiors in the fusion zone to become more homogeneous with less of a solute gradient. The local peak in HAZ hardness also disappears. Artificial aging after SHT (Fig. 5) hardens the weldments even more by allowing greater precipitation hardening to occur, although lower ductility is found at long aging times as grain boundaries become more decorated in both the fusion zone and the HAZ.

Tensile Tests: As-Welded, Ambient Temperature

The strength values reported are among the highest values found in the

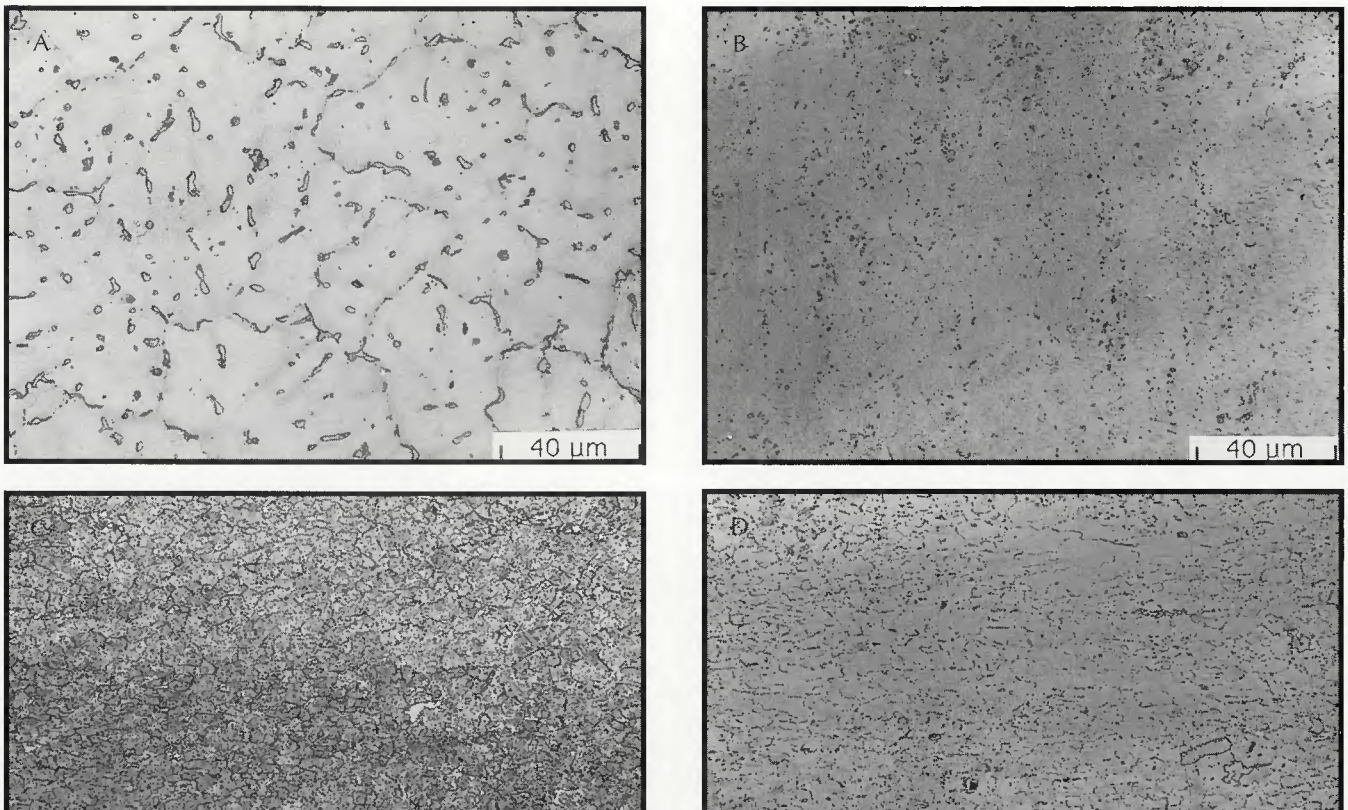

Fig. 4 — Microstructure of: A — weld metal (filler metal 5Cu-1Li); B — the hard region of the HAZ; C — the soft region of the HAZ; D— the unaffected base metal.

literature, and the ductility values obtained are good for such high strengths. Very few Al alloys are capable of exceeding a tensile strength of 300 MPa in arc-welded weldments without post-weld heat-treatment.

The weldment tensile specimens typically failed through the weld metal and the corner of the HAZ — Fig. 6. Fracture is primarily interdendritic, and the intermetallic phases decorate each fracture surface — Fig. 7. These intermetallics are brittle, as evidenced by their being cracked near the fracture surface.

The fracture surfaces of the ternary filler metal weldments are heavily dimpled, which are consistent with the high reduction in area measured — Fig. 8. Also evident is secondary cracking along dendrite boundaries and remnants of intermetallic phases.

Tensile Tests: Cryogenic Temperature

Tensile specimens tested at –196°C show a dramatic strength increase but were less ductile than those tested at

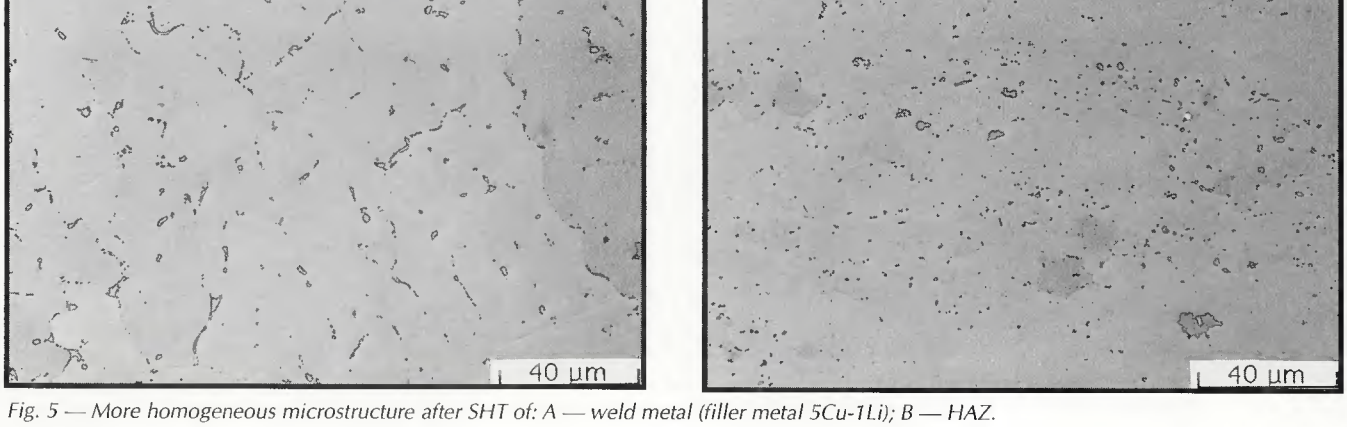

Fig. 5 — More homogeneous microstructure after SHT of: A — weld metal (filler metal 5Cu-1Li); B — HAZ.

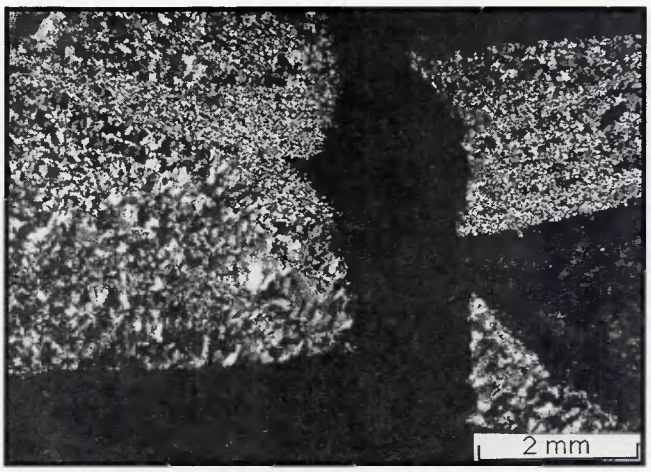

Fig. 6 — Tensile fracture through the weld and HAZ corner of an as-welded specimen.

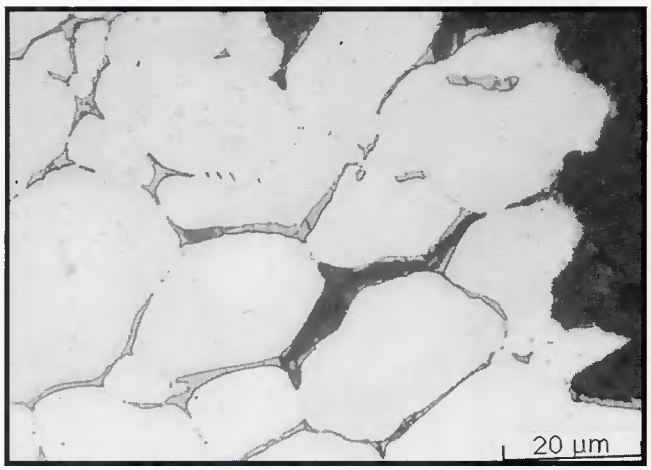

Fig. 7 — Brittle intermetallic phases at the fracture surface of a weld tensile specimen.

20°C. The differences in mechanical properties between the various filler metal weldments seem to be amplified at this low temperature. For example, weldments made with 5Cu-0.5Li and 2319 filler metals have a lower UTS, whereas those made using 5Cu-1.5Li filler metal suffer from lower ductility. Weldments made with 5Cu-1Li filler metal display the best combination of strength and ductility. The strength differences are consistent with the fracture paths observed, with the lower strength weldments occasionally failing through the center of the weld bead. The higher strength weldments failed through the weld metal and the corner of the HAZ, as was the case at 20°C. The weldments made with 5Cu-1.5Li filler metal contain more Li, and copious amounts of brittle intermetallic phases form during solidification, which may account for the lower ductility found at lower temperatures. In general, SEM fractographs are comparable with those of ambient temperature specimens, with ductility and secondary cracking along dendrite boundaries still evident — Fig. 9. A similar fracture mode at 25°C (77°F) and –196°C with retention of ductility is an important attribute. Certain alloy/filler metal weldment combinations change from a ductile fracture mode at room temperature to a brittle intergranular or quasicleavage mode at cryogenic temperatures (Ref. 14).

Tensile Tests: Heat-Treated Condition

A cursory postweld aging study was performed on the 5Cu-1Li filler metal weldment, with aging time varied at 160°C. Initially, strength decreases slightly upon aging with a corresponding increase in ductility — Table 4. This "reversion" phenomena has been studied by Gayle, *et al.* (Ref. 13), in Weldalite 049 extruded bar, and it results from the dissolution of small δ′ (Al_3Li) precipitates and some GP zones formed during natural aging. The present results suggest that a short, elevated temperature aging treatment may be an effective method for obtaining increased weldment ductility without a full SHT. Continued artificial aging increases the yield strength, but no major increase in UTS is realized without a significant loss of ductility. The fracture surface contains some dimpling, but with sharper and more abundant cell boundary cracks — Fig. 10.

Artificial aging after SHT causes an immediate strength drop due to reversion, with a corresponding increase in ductility. Continued aging increases the strength, eventually above 600 MPa, while decreasing the ductility. It should be noted that most base metal aluminum alloys cannot attain this high strength level even in the fully heat-treated, unwelded condition. The aging response is similar to that of the base metal (Ref. 15) and a good strength-to-ductility ratio is similarly found at a slightly underaged (*i.e.*, less than 40 h) condition. Overaging produces an abundance of grain boundary and coarse matrix precipi-

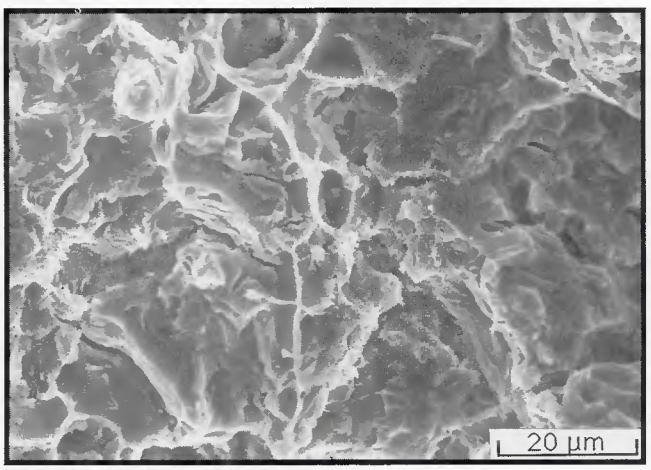

Fig. 8 — Scanning electron fractograph of an as-welded tensile fracture shows a dimpled surface with secondary boundary cracking.

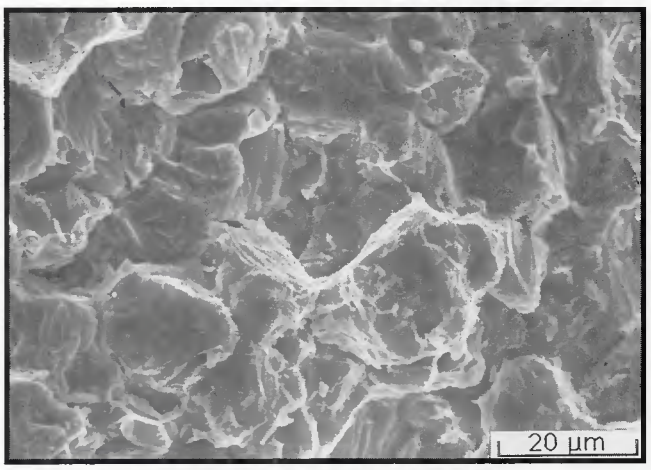

Fig. 9 — Scanning electron fractograph of a cryogenic (–196°C) tensile specimen.

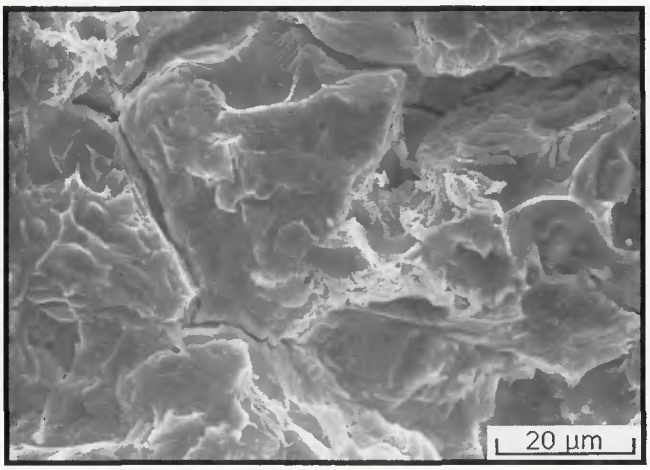

Fig. 10 — Scanning electron fractograph of a postweld aged tensile specimen reveals cracking at the cell boundaries.

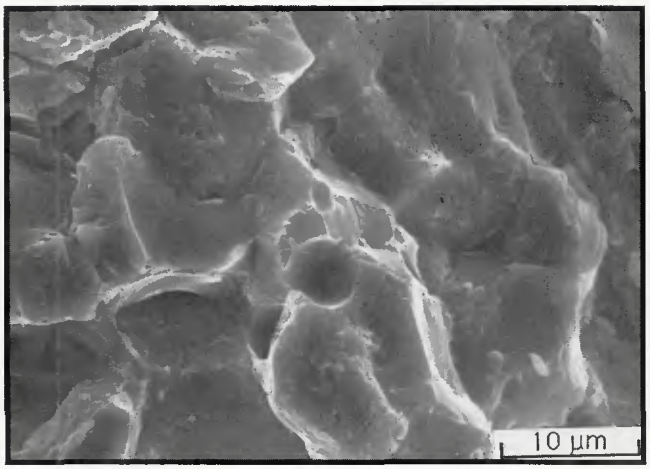

Fig. 11 — Dimpling and a more homogeneous microstructure are evident in this scanning electron fractograph of a solution heat-treated and aged tensile specimen.

tates, that are detrimental to ductility. The fracture surface after SHT (Fig. 11) resembles those in the as-welded condition, but with some differences. The fracture is ductile, but there is less of a stepped surface appearance within the grains (compare with Fig. 8). This is possibly due to the disappearance of much of the interdendritic intermetallic phases during SHT, causing a more homogeneous distribution of solute.

Conclusions

1) Weldalite™ 049 is capable of porosity- and crack-free weldments that exhibit very high tensile properties.

2) Of the three Li-containing filler metals tested, the Al-5.2Cu-1Li variant exhibited the best combination of strength and ductility: as-welded tensile strengths of 50.8 ksi (350 MPa) with 10% RA at 20°C, and 58.7 ksi (405 MPa) with 5.4% RA at –196°C.

3) For the variable polarity welding process examined, the dilution of base metal into the weld zone provides sufficient amounts of grain-refining elements to give fine-grained, high-strength weldments without additional grain refiners added via the filler metal.

4) The SHT and aging of these weldments produce a more homogeneous and refined microstructure, which accounts for the increased hardness and high tensile values.

5) Artificial aging of the weldments (*i.*e., without re-SHT) increases weldment ductility without a significant strength penalty.

Acknowledgments

The authors wish to thank Dr. C. E. Cross, and L. W. Loechel for their helpful comments and R. Zibilich for providing the quality weldments, all of Martin Marietta Astronautics Group, Denver Colo. This work was in part supported by the Martin Marietta Emerging Technologies Fund.

References

1. Pickens, J. R., Heubaum, F. H., Langan, T. J. and Kramer, L. S. 1989. Proc. Fifth International Aluminum-Lithium Conf. T. N. Sanders and E. A. Starke, eds., MCE Publications Ltd., Birmingham, U.K. pp.1397–1414.

2. Tack, W. T., and Loechel, L. W. ibid., pp. 1457–1468.

3. Cross, C. E., Olson, D. L., Edwards, G. R., and Capes, J. F. 1986. Proc. Conf. Al alloys: their physical and mechanical properties. Charlottesville, Va., pp. 1869–1875.

4. Kramer, L. S., Heubaum, F. H., and Pickens, J. R. op. cit. Ref. 1, pp. 1415–1429.

5. Pickens, J. R. 1990. *J. Mater. Sci.* 25, pp. 3035–3047.

6 Yunjia, H., Frost, R. H., Olson, D. L., and Edwards, G. R. 1988. *Welding Journal* 68(7): 280-s to 289-s..

7. Ganaha, T., and Pearce, B. P. 1980. Metall. Trans. 11A, pp. 1351–1359.

8. Davies, G. J., and Garland, J. G. 1975. Int. Met. Rev. 20, pp. 83–106.

9. Brown, P. E., and Adams, C. M., Jr. 1960. *Welding Journal* 39(8): 520-s to 524-s.

10 Kou, S. 1986. *WRC Bulletin* 320, pp. 1–20.

11. Ischenko, A. Ya., and Lozovskaya, A. V. 1980. Avt. Svark. pp. 29–31.

12. Kumar, K. S., Brown, S. A., and Pickens, J. R. 1990. *Scripta Metall.* 24, pp. 1245–1250.

13. Gayle, F. W., Heubaum, F. H., and Pickens, J. R. op. cit. Ref. 1, pp. 701–710.

14. Sunwoo, A. J., and Morris, J. W., Jr. 1989. *Welding Journal* 68(7): 262-s to 268-s.

15. Pickens, J. R., Heubaum, F. H., and Kramer, L. S. 1990. *Scripta Metall.* 24, pp. 457–462.

WRC Bulletin 343
May 1989

Destructive Examination of PVRC Weld Specimens 202, 203 and 251J

This Bulletin contains three reports:

(1) Destructive Examination of PVRC Specimen 202 Weld Flaws by JPVRC
By Y. Saiga

(2) Destructive Examination of PVRC Nozzle Weld Specimen 203 Weld Flaws by JPVRC
By Y. Saiga

(3) Destructive Examination of PVRC Specimen 251J Weld Flaws
By S. Yukawa

The sectioning and examination of Specimens 202 and 203 were sponsored by the Nondestructive Examination Committee of the Japan Pressure Vessel Research Council. The destructive examination of Specimen 251J was performed at the General Electric Company in Schenectady, N.Y., under the sponsorship of the Subcommittee on Nondestructive Examination of Pressure Components of the Pressure Vessel Research Committee of the Welding Research Council. The price of WRC Bulletin 343 is $24.00 per copy, plus $5.00 for U.S., or $8.00 for overseas, postage and handling. Orders should be sent with payment to the Welding Research Council, Room 1301, 345 E. 47th St., New York, NY 10017.

WRC Bulletin 354
June 1990

The two papers contained in this bulletin provide definitive information concerning the elevated temperature rupture behavior of 2¼Cr-1Mo weld metals.

(1) Failure Analysis of a Service-Exposed Hot Reheat Steam Line in a Utility Steam Plant
By C. D. Lundin, K. K. Khan, D. Yang, S. Hilton and W. Zielke

(2) The Influence of Flux Composition of the Elevated Temperature Properties of Cr-Mo Submerged Arc Weldments
By J. F. Henry, F. W. Ellis and C. D. Lundin

The first paper gives a detailed metallurgical failure analysis of cracking in a longitudinally welded hot reheat pipe with 184,000 hours of operation at 1050°F. The second paper defines the role of the welding flux in submerged arc welding of 2¼Cr-1Mo steel.

Publication of this report was sponsored by the Steering and Technical Committees on Piping Systems of the Pressure Vessel Research Council of the Welding Research Council. The price of WRC Bulletin 354 is $50.00 per copy, plus $5.00 for U.S. and $10.00 for overseas postage and handling. Orders should be sent with payment to the Welding Research Council, 345 E. 47th St., Room 1301, New York, NY 10017.